Untangling the adolescent internalizing brain: investigations on brain networks in youth with anxious and depressive problems

Roelofs, E.F.


Part 2

4

Investigating microstructure of white matter tracts as candidate endophenotypes of Social Anxiety Disorder – findings from the Leiden Family Lab study on Social Anxiety Disorder (LFLSAD)

Eline F. Roelofs, Janna Marie Bas-Hoogendam, Hanneke van Ewijk, Habib Ganjgahi, Steven J.A. van der Werff, Marjolein E.A. Barendse, P. Michiel Westenberg, Robert R.J.M Vermeiren, Nic J.A. van der Wee

Neuroimage Clin 2020 Vol. 28 Pages 102493

Abstract

Background: Social anxiety disorder (SAD) is a mental illness with a complex, partially genetic background. Differences in characteristics of white matter (WM) microstructure have been reported in patients with SAD compared to healthy controls. Also, WM characteristics are moderately to highly heritable. Endophenotypes are measurable characteristics on the road from genotype to phenotype, putatively reflective of genetically based disease mechanisms. In search of candidate endophenotypes of SAD we used a unique sample of SAD patients and their family members of two generations to explore microstructure of WM tracts as candidate endophenotypes. We focused on two endophenotype criteria: co-segregation with social anxiety within the families, and heritability.

Methods: Participants (n = 94 from 8 families genetically vulnerable for SAD) took part in the Leiden Family Lab Study on Social Anxiety Disorder (LFLSAD). We employed tract-based spatial statistics to examine structural WM characteristics, being fractional anisotropy (FA), axial diffusivity (AD), mean diffusivity (MD) and radial diffusivity (RD), in three a-priori defined tracts of interest: uncinate fasciculus (UF), superior longitudinal fasciculus (SLF) and inferior longitudinal fasciculus (ILF). Associations with social anxiety symptoms and heritability were estimated.

Results: Increased FA in the left and right SLF co-segregated with symptoms of social anxiety. These findings were coupled with decreased RD and MD. All characteristics of WM microstructure were estimated to be at least moderately heritable.

Conclusion: These findings suggest that alterations in WM microstructure in the SLF could be candidate endophenotypes of SAD, as they co-segregated within families genetically vulnerable for SAD and are heritable. These findings further elucidate the genetic susceptibility to SAD and improve our understanding of the overall etiology.

Introduction

Social anxiety disorder (SAD) is a highly prevalent mental illness with a typical onset during late childhood and early adolescence [1]. Patients with SAD experience an excessive fear of negative evaluation in social situations, which are either avoided or endured with intense fear or anxiety [2]. SAD often has a chronic course and high comorbidity rates with other mental disorders [3-8]. Unfortunately, the wide range of cognitive behavioral and pharmacological therapies available proves to be insufficient in 30 – 40% of patients [9]. To improve current therapies and develop new interventions, the etiology of SAD should be further elucidated [10, 11].

In the past decades, research into the neurobiological background of mental disorders has increased and evolved, with a special interest in neuroimaging of the brain. Indeed, several mental disorders, including SAD, have been associated with altered brain functioning [11, 12]. For example, previous research in patients with SAD has reported abnormalities in the activity of the anxiety circuitry and its regulatory networks, such as hyperactivation of the amygdala and insula in relation to negative emotional stimuli [13] and decreased functional coupling between the amygdala and regulatory prefrontal cortical regions such as the orbitofrontal cortex [14]. In addition, altered resting state functional connectivity has been reported, such as decreased connectivity between the amygdala and frontal regions such as the medial, dorsolateral and ventrolateral prefrontal cortex (PFC) and between regions implicated in the default mode network like the medial PFC and the lateral parietal cortex (reviewed in MacNamara *et al.* [15]).

A recent neurofunctional model on SAD suggested disturbed emotion regulation networks in patients with SAD, with an imbalance between hyperactive parietal and medial occipital brain regions and fear circuitry on the one hand, and impairments in regulatory control networks in frontal areas on the other hand. This imbalance might be partly attributed to impaired communication between these areas due to decreased structural connectivity, such as abnormal microstructure of several white matter (WM) tracts [11].

A method to study characteristics of WM microstructure of the brain is diffusion tensor imaging (DTI), which in turn can be utilized to model four commonly used scalar measures of diffusivity: fractional anisotropy (FA), axial diffusivity (AD), radial diffusivity (RD) and mean diffusivity (MD). Differences in microstructure of several WM tracts, such as the uncinate fasciculus (UF), superior longitudinal fasciculus (SLF) and inferior longitudinal fasciculus (ILF), have been reported frequently in Magnetic Resonance Imaging (MRI) studies in SAD. For an overview of current literature on DTI studies in SAD, see Supplemental Table 1a and 1b, summarizing the work by Jenkins *et al.* [12], Tukel *et al.* [16], Qiu *et al.* [17], Phan *et al.* [18], Liao *et al.* [19], [20], Baur *et al.* [21]. The UF connects the prefrontal cortex with the anteromedial temporal lobe and is thought to be, among others, involved in social emotional processing [22]. In voxelwise analyses, decreased FA of the left and right UF has been previously reported in SAD patients compared to healthy controls [17, 18, 21] and one study replicated these results using tractography analyses [20]. The SLF is roughly divided in three subparts (I, II and III) and is the major tract connecting parietal cortices to prefrontal areas [23]. It is thought to subserve visuo-spatial attention

and language functionality [24], and in voxelwise studies decreased FA of the left SLF has been reported in patients with SAD [16, 21]. Interestingly, this finding was replicated in a voxelwise meta-analysis of FA [12]. The ILF originates from medial and lateral anterior temporal areas and terminates in the occipital lobe. This tract is suggested to play a role in facial recognition [25-27] and one voxelwise study reported decreased FA in patients with SAD compared to healthy controls [16]. Interestingly, when using a tract-of-interest (TOI) approach, an increase in average FA of the bilateral UF and right ILF has been reported after 10 weeks of cognitive behavioral group therapy [28] and higher values of a combined tractography measure of AD, MD, RD and FA of the right ILF has been found to predict better clinical response to cognitive behavioral therapy in individual and group settings [29]. Also, an inverse voxelwise relation between FA in a putative amygdala-prefrontal pathway and trait anxiety has been reported [30, 31]. Interestingly, the three WM tracts mentioned above are also thought to be involved in several resting-state functional brain regions and networks in which altered connectivity has been reported in SAD patients, such as regions involved in the DMN, the ventral attention network and the fronto-parietal network, [15, 32, 33]. These results suggest that abnormal WM microstructure, together with other underlying neurobiological processes, could be linked to SAD.

It is thought that the overall vulnerability to develop SAD is based on complex interactions between genetic (dis)advantages and liabilities, epigenetic factors and environmental factors [1, 34, 35]. For example, studies using twins and families indicated that genetic and non-shared environmental factors explained roughly equally most of the individual differences in SAD [36] and a recent genome wide association study (GWAS) analysis confirmed a heritable basis of SAD [37]. To study the genetic vulnerability to SAD more closely, an endophenotype approach could be used. Endophenotypes are defined as biological or psychological markers of a disorder, which are thought to be in the causal chain between genetic contributions to a disorder and diagnosable symptoms of psychopathology [38, 39]. The endophenotype approach assumes that underlying measurable components of a mental illness are heritable and present before the development of clinical symptoms and include, for example, neurobiological changes in brain structure and function. It is thought that endophenotypes are theoretically capable of providing greater statistical power to localize and identify disease related biomarkers than affection status alone [40]. To be considered an endophenotype, a candidate psychoneurobiological characteristic has to be associated with the disorder (criterion 1), state-independent (criterion 2), heritable (criterion 3) and co-segregate with the disorder within families of probands whilst already present in a preclinical state (criterion 4) [38, 39, 41, 42].

Several neurobiological candidate endophenotypes for SAD have been proposed, such as WM and grey matter (GM) characteristics, amygdala and prefrontal brain function and alterations in functional connectivity networks [43]. The Leiden Family Lab study on Social Anxiety Disorder (LFLSAD) is to our knowledge the first comprehensive two-generation family neuroimaging study on SAD and has been designed specifically to examine the heritability and first part of the co-segregation criteria of candidate endophenotypes of SAD [44]. Previous results of this study suggest that several characteristics of brain structure and function, like cortical and subcortical GM characteristics, increased and

prolonged amygdala activation, and increased brain activity whilst processing unintentional social norm violations, could be endophenotypes of SAD [45-49]. However, it still remains to be elucidated whether characteristics of WM microstructure could be candidate endophenotypes of SAD. Results of previous studies suggest that this could indeed be the case, as they were found to be associated with the disease in case-control studies (endophenotype criterion 1) and are at least moderately ($h^2 \geq 0.2$) to highly ($h^2 \geq 0.6$) heritable as shown by multiple studies in healthy twins (endophenotype criterion 3) [50, 51]. However, to our knowledge the criterion of co-segregation within families of probands (criterion 4, first element) has not been examined in previous work.

Using DTI data from the LFLSAD, the present study investigated characteristics of WM microstructure as candidate endophenotypes of SAD, with a focus on: 1) co-segregation within families genetically enriched for SAD and 2) estimation of heritability of WM characteristics. We employed tract-based spatial statistics (TBSS; [52]) to examine the association between measures of WM microstructure and measures of social anxiety. Our main parameter of interest was FA, while we used other parameters, being AD, MD and RD, to gain more insight into underlying WM microstructure (cf. van der Werff *et al.* [53], Aghajani *et al.* [54]). Based on previous research we expected to find a negative association between the level of social anxiety symptoms and FA and AD in the UF, SLF and ILF, coupled with a positive association between clinical symptoms and RD and MD. Furthermore, we expected estimates of all WM parameters to be at least moderately heritable. We employed a-priori defined TOI analyses in these three tracts using two types of analyses: a voxelwise analysis and an analysis of the averaged values of WM parameters over the whole TOI. In addition, we performed an exploratory voxelwise analysis of the whole WM skeleton to investigate WM microstructure outside the a-priori defined regions.

Methods and Materials

Participants

The LFLSAD is a multiplex (families were selected based on a minimum of two (sub)clinical SAD cases within one nuclear family) and multigenerational (multiple nuclear families encompassing two generations from the same family participated) family study on SAD (total sample: n = 132, from nine families, MRI participants n = 113), designed to investigate candidate neurobiological endophenotypes of SAD. A design like this is especially powerful to investigate environmental and genetic influences on SAD-related characteristics [44]. The background, objectives and methods as well as clinical characteristics of the sample and an a priori power analysis are described in more detail elsewhere [44]. Preregistration of the study is available on https://osf.io/e368h. The LFLSAD sample consists of families selected on presence of a primary diagnosis of SAD in a parent (25 – 55 years old; 'proband'), with a child who met the criteria for clinical or subclinical SAD (living at home, 8 – 21 years old; 'proband's SA child'). Furthermore, the partner of the proband, other children of this nuclear family (≥ 8 years of age), siblings of the proband and their partners and children (≥ 8 years of age) were invited to participate. Thus, the sample consisted of two generations of family members: the generation

of the proband (generation 1) and the generation of the proband's SA-child (generation 2; see Figure 1). Exclusion criteria for the proband or proband's SA child were comorbidity other than internalizing disorders; other family members were included regardless of the presence of psychopathology. Exclusion criteria for all participants for the MRI experiment were general MRI contraindications, such as metal implants or pregnancy.

MRI data from one family (n = 3 family members) had to be excluded from the present analysis as the proband from this family was not able to participate in the MRI experiment due to an MRI contraindication. DTI data from two subjects (9.4 y and 18.5 y) were not available due to an early stop of data acquisition during the MRI experiment, which consisted of several structural and functional scans as described elsewhere (total duration of the MRI protocol: 54 min 47 s) [44]. Thus, data from n = 108 participants was available for initial DTI analysis.

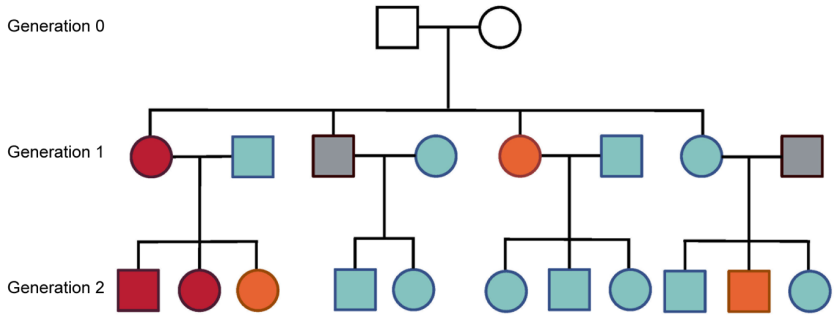

Figure 1 Family structure in the LFLSAD. Example of a family within the Leiden Family Lab study on Social Anxiety Disorder. Families were included based on the combination of a parent with social anxiety disorder (SAD; "proband": depicted in red) and a proband's child with SAD (red) or (sub)clinical SAD (orange). In addition, family members of two generations were invited, independent from the presence of SAD within these family members (no SAD: light blue; did not participate: gray). Grandparents (Generation 0; white) were not invited for participation. This family is slightly modified to guarantee anonymity; however, the number of family members and the frequency of (sub)clinical SAD are depicted truthfully. Squares and circles represent men and women, respectively. This figure is a reprint of the figure published in [44].

Ethics

The LFLSAD study was approved by the Medical Ethical Committee of the Leiden University Medical Center (P12.061). All participants provided informed consent according to the Declaration of Helsinki; both parents signed the informed consent form for their children, while children between 12 and 18 years of age signed the form themselves as well.

Phenotyping

Confinement of diagnosis

To determine the presence of DSM-IV diagnoses, with special attention to SAD, the Mini-International Neuropsychiatric Interview (MINI)-Plus (version 5.0.0) or MINI-Kid (version 6.0) was used by experienced clinicians and was voice-recorded for review [55-58]. Diagnosis of clinical SAD was

determined using the DSM-IV-TR criteria for the generalized subtype of SAD, but a clinician verified that DSM-5 criteria were also met to establish the diagnosis. Subclinical SAD was diagnosed when DSM-5 criteria were met, but important areas of functioning were not impaired (criterion G) [2].

Questionnaires

All participants completed self-report questionnaires regarding anxiety-related symptoms. If applicable, age-appropriate questionnaires were used. Among others, we measured social anxiety symptoms, using the Liebowitz Social Anxiety Scale (LSAS-SR) for adults (≥ 18 years of age) [59, 60] and the Social Anxiety Scale for Adolescents (SAS-A) for younger participants (< 18 years of age) [61], the intensity of fear of negative evaluation using the revised Brief Fear of Negative Evaluation (BFNE – II scale) [62, 63] and the level of trait anxiety using the State-Trait Anxiety Inventory (STAI) [64]. Furthermore, depressive symptoms were evaluated by the self-report Beck Depression Inventory (BDI-II) for adults [65, 66] or the Children's Depression Inventory (CDI) for adolescents [67]. To analyze the scores of the age-appropriate self-report questionnaires, z-scores were computed for the level of social anxiety symptoms and depressive symptoms as described previously [44].

Incidental missing values on the self-report questionnaires were replaced by the mean value of the completed items. Data on the BFNE-II was missing for one participant. Differences in scores on self-report questionnaires between participants with (sub)clinical SAD and non-affected relatives were assessed by fitting regression models in R [68]. Within these models, outcomes from self-report questionnaires (levels of social anxiety symptoms (z-score; z-SA), intensity of fear of negative evaluation (FNE), depressive symptoms (z-score) and trait anxiety) were modelled as dependent variables and (sub) clinical SAD as independent variable. Genetic correlations between family members were accounted for by including random effects in the models, and gender and age (centered) were added as covariates. The Bonferroni method was used to correct p-values for multiple comparisons (4 tests, corrected p-value = 0.0125).

MRI data acquisition

Scanning was performed at Leiden University Medical Center using a 3.0T Philips Achieva MRI scanner (Philips Medical Systems, Best, The Netherlands), equipped with a 32-channel Sensitivity Encoding (SENSE) head coil. The MRI session consisted of several structural and functional scans, as described elsewhere (total duration of the MRI protocol: 54 min 47 s) [44]. Of interest for the present study are two diffusion weighted imaging (DWI) scans with the following characteristics: repetition time (TR) 7316 ms, echo time (TE) 69 ms, field of view (FOV) 240 x 240 x 150 mm, acquisition matrix 128 x 128 with 75 slices, slice thickness 2 mm, voxel size 1.9 x 2.4 mm. DWI scans (b = 1000 s/mm^2) were acquired in 30 directions with two additional non-DWI scans (b = 0 s/mm^2) serving as reference scans. The two DWI scans were collected with reversed phase-encode blips, resulting in pairs of images with distortions going in opposite directions (anterior-posterior and posterior-anterior). Scan duration for each scan was about 4 min 30 s. Furthermore, one high-resolution T1-weighted structural scan was acquired with the following characteristics: 140 slices, resolution 0.875 mm × 0.875 mm × 1.2 mm, FOV = 224 mm × 168

mm × 177.333 mm, TR = 9.8 ms, TE = 4.59 ms, flip angle = 8°. All structural MRI scans were inspected by a neuroradiologist. No clinically relevant characteristics were reported in any of the participants.

Data analysis

DTI processing

DTI models diffusivity of water molecules across the brain, using tensors. These tensors consist of three main eigenvalues (λ_1, λ_2 and λ_3) which in turn can be used to calculate the four most commonly used characteristics of WM microstructure: fractional anisotropy (FA), axial diffusivity (AD), radial diffusivity (RD), and mean diffusivity (MD) [69]. FA provides a relative difference between the largest eigenvalue as compared to the others, reflecting the tendency of water molecules to diffuse in one direction as opposed to all others and could therefore be described as a general indicator for WM microstructure (e.g. myelin thickness, membrane integrity) [69, 70]. AD is defined as the first eigenvalue (l_1) and reflects water diffusion along the principal direction of the fiber, displaying fiber bundle coherence and axonal integrity [71]. RD is defined as the average of the second and third eigenvalue (λ_2 and λ_3) and reflects water diffusion perpendicular to the principal direction of the fiber, thus being more indicative of the level of myelinization [72]. MD is defined as the average of the three eigenvalues and hence reflects average water diffusion in all directions within a fiber, thus putatively reflective of a degree of myelination [73]. In general, decreased FA is coupled with decreased AD and / or increased RD and MD and vice versa [69, 74].

Image pre-processing and analyses were performed using the Oxford Centre for Functional Magnetic Resonance Imaging of the Brain (FMRIB) Software Library (FSL) [75]. The susceptibility-induced off-resonance field from the two pairs of DWI images was estimated using a method similar to that described in [76] and the two images were combined into a single corrected one. Afterwards, the Brain Extraction Tool (BET) was used to remove non-brain tissue from the non-diffusion images [77]. Image distortion and motion artefacts induced by eddy currents or inter-volume head motions were corrected [78] and image quality was statistically evaluated afterwards [79]. No outliers were detected. Individual FA images and primary (l_1), secondary (l_2) and tertiary (l_3) eigenvalues were created by fitting a tensor model to the raw diffusion data using FMRIB's Diffusion Toolbox (FDT) [80]. Individual maps of other diffusivity measures were calculated out of eigenvalues, defining AD as l_1, RD as $l_{23} = (l_2 + l_3) / 2$ and MD as $l_{123} = (l_1 + l_2 + l_3)/3$. The individual vector and raw FA images were visually and statistically evaluated for alignment on WM tracts according to standardized protocols, designed to facilitate harmonized image analysis across multiple sites (http://enigma.ini.usc.edu/protocols/dti-protocols/).

Then, a study-specific custom FA template was created. All subjects' FA data were slightly eroded and aligned into a common space using the nonlinear registration tool FNIRT [81, 82], which uses a b-spline representation of the registration warp field [83]. Afterwards, a mean FA image and distance map to the masked template were created. Individual FA and non-FA (AD, MD and RD) images were then projected onto the template. Subsequently, quality control was performed twofold: we visually inspected the registered images for misalignment onto the skeleton, and individual projection distances of the

extracted skeletons onto the template were calculated to detect outliers (defined as individual projection distance to the template exceeding the threshold of 3.8 mm), which could represent bad alignment to the template [84]. All images were well aligned, and no outliers were detected.

Investigation of WM candidate endophenotypes

We focused on two endophenotype criteria: (i) co-segregation of the candidate endophenotypes with the disorder within families (the first element of criterion 4) and (ii) heritability estimation (h^2) of characteristics of WM microstructure (criterion 3). Co-segregation of WM characteristics within families was examined by exploring the relationship between parameters of WM microstructure and two-dimensional measures of social anxiety (z-SA and FNE) using three a priori defined WM tracts based on previous literature: the SLF, ILF and UF (see Supplemental Figure 1 for TOIs, for an overview of current literature, see Supplemental Table 1a and 1b). To investigate WM microstructure outside the a-priori defined regions, we also examined the association between WM parameters and a diagnosis of (sub)clinical SAD (see Supplemental section).

Selection of tracts

Binary unilateral masks of the SLF, UF and ILF were created using the probabilistic Johns Hopkins University (JHU) white-matter tractography atlas [85] provided by FSL, thresholded at a conventional 20% [52]. Using the mean FA skeleton, each tract was unilaterally masked to include only voxels comprised in both the tract and the skeleton. This confines the statistical analysis to voxels from the center of the tract, thereby minimizing anatomic intersubject variability, deviations in registration and partial volume effects [86].

Co-segregation

To examine co-segregation of WM characteristics, voxelwise and average TOI analyses were conducted. We report findings uncorrected for the number of tracts because of the use of a priori defined TOIs, which are possibly also functionally related [87] and because of the innovative and more explorative nature of the present study (to the best of our knowledge, this is the first comprehensive family study on SAD). To investigate WM microstructure outside the a-priori defined regions, an exploratory analysis was conducted to investigate voxelwise associations between FA in the WM skeleton and the level of self-reported symptoms of SAD was conducted using NINGA (see Supplemental section for more details and results).

For the voxelwise and average TOI analyses, sensitivity analyses were conducted to control for (i) psychopathology other than SAD and (ii) severity of depressive symptoms. Therefore, all participants with past and/or present (comorbid) psychopathology other than SAD were excluded (sensitivity analysis 1); or the z-score of the level of depressive symptoms was added as a covariate in the analyses (sensitivity analysis 2). Details and results of these analyses are included in the Supplemental section.

Voxelwise TOI analysis

First, we performed voxelwise analyses within each of the TOIs to examine subtle localized differences which could disappear in average TOI analyses due to the size of the TOI. In these voxelwise TOI analyses, FA was used as principal outcome measure as this is a general indicator of WM microstructure. Additional WM parameters, being AD, MD and RD, were examined for significant clusters only, to provide complementary information about WM microstructure and to aid interpretation of FA changes. The voxelwise TOI analyses were conducted by performing multiple nonparametric regression analyses using the NeuroImaging Nonparametric Genetic Analysis (NINGA) toolbox [88, 89] as methods previously used in analyses of fMRI data of the LFLSAD could, due to the specific structure of TBSS data and assumptions regarding the random field theory, not account for family-wise errors (FWE). NINGA implements linear mixed effect for covariate inference in presence of family relatedness using an approximate non-iterative random effect estimator based on restricted maximum likelihood function. It uses permutation test to provide essential spatial statistics inference tools for uncorrected and family-wise error (FWE) corrected p-values. Individual levels of self-reported social anxiety (z-SA and FNE) were modelled as independent variables and voxelwise FA values as the dependent variable. Covariate inference was incorporated in the model to account for nuisance kinship, gender and age. We used Threshold-Free Cluster Enhancement (TFCE) statistics to define significant clusters, and permutation testing to provide FWE corrected p-values at a conventional threshold of a= 0.05.

To gain more insight in the direction of FA in clusters displaying significant associations with SA-symptoms, RD, MD and AD were examined by extracting and binarizing the significant cluster from the previous analysis. This mask was then used to comprise only the relevant voxels in individual skeletons of AD, MD and RD. Next, individual levels of self-reported social anxiety symptoms (z-SA and FNE) were modelled as independent variables and values of AD, MD or RD in the relevant cluster as the dependent variable. Covariate inference was incorporated to account for nuisance kinship, gender and age.

Average TOI analysis

Second, we conducted conventional TOI analyses using average individual values of WM parameters over the whole tract to allow comparison with previous literature ("average TOI analyses") and to ensure continuity with previous analyses performed on data from the LFLSAD [45].That is, following methods previously described [45-47, 49], associations between individual average values of WM parameters (FA, MD, RD and AD over the whole tract) per tract and clinical symptoms of SAD (z-SA and FNE) were examined by performing multiple regression analyses using linear mixed models in R [68]. Average values of FA, AD, MD and RD were extracted for each individual unilaterally per tract. Per TOI, mean WM parameters were modelled as dependent variables and the outcomes of self-report questionnaires as independent variables. Correlations between family members were accounted for by including random effects in the models [90]. Both age (centered) and gender (centered) were included as covariates. As most of the dependent variables were non-normally distributed, the robustness of the linear mixed model used was confirmed by checking the distribution of the residuals of the phenotypes with the Shapiro-

Wilk normality test and visual inspection, which showed all residuals followed an approximate normal distribution.

Heritability

Next, general heritability (h^2) of the WM microstructure characteristics was estimated, using methods previously used in analyses of the LFLSAD sample to ensure consistency [45-49]. This method estimates heritability by jointly modelling SAD status and the individual average values of FA, AD, MD, and RD within all TOIs in a multivariate-mixed probit model, by which the familial relationship and ascertainment of the families (based on SAD in the proband and (sub)clinical SAD in the proband's SA-child) were taken into account [90]. To adjust for age and gender, these variables were included as covariates (both centered) in the marginal regression models. Variance of the random effects was determined using maximum-likelihood estimates; subsequently, heritability was estimated [90].

Results

Sample characteristics

Sample characteristics are summarized in Table 1. Participants with (sub)clinical SAD reported significantly higher levels of social anxiety (self-reported social anxiety symptoms (z-SA) and FNE), depressive symptoms and trait anxiety compared to their non-SAD relatives but did not differ with respect to gender-distribution, generation, age or IQ. For a more elaborate description of this sample, including diagnostic information and details on quality checking and data availability, we refer to the Supplemental section and previous publications on the LFLSAD in general [44] and the MRI sample in particular [45-47, 49].

Table 1 Characteristics of participants with and without (sub)clinical SAD.

	(Sub)clinical SAD (n = 31)	No SAD (n = 57)	Statistical analysis
Demographics			
Male / Female (n)	13 / 18	28 / 29	$c^2 = 0.42$, p = .52
Generation 1 / Generation 2 (n)	19 / 12	27 / 30	$c^2 = 1.56$, p = .21
Age in years (mean ± SD); range	33.7 ± 15.5 (9.2 - 59.6)	32.9 ± 14.8 (9.6 - 61.5)	b ± SE = 0.8 ± 3.3, p = .80
Estimated IQ (mean ± SD)	102.2 ± 12.2	105.5 ± 10.8	b ± SE = -3.1 ± 2.4, p = .21
Diagnostic information (n)			
Clinical SAD	15	0	$c^2 = 33.3$, p < .001**
Self-report measures (mean ± SD)			
Social anxiety symptoms (z-score)	2.4 ± 3.3	0.7 ± 1.3	b ± SE = 1.9 ± 0.5, p < .001**
FNE	23.0 ± 12.4	12.0 ± 7.6	b ± SE = 10.6 ± 2.2, p < .001**
Depressive symptoms (z-score)	0.05 ± 0.9	-0.6 ± 0.6	b ± SE = 0.6 ± 0.2, p = .001**
Trait anxiety	38.0 ± 9.8	33.2 ± 8.6	b ± SE = 5.0 ± 2.0, p = .01*

SAD: social anxiety disorder; FNE: fear of negative evaluation; STAI: state-trait anxiety inventory; SD: standard deviation. Sample for dimensional analysis: n = 94 for z-SA, n = 93 for FNE. Data on the presence of subclinical SAD were, due to technical reasons, lost for six family members (remaining sample for categorical analysis: n = 88). ** significant at Bonferroni corrected p-value of 0.0125; * significant at uncorrected p-value of 0.05.

Co-segregration

Three bilateral TOIs were examined in voxelwise and average TOI analyses to explore the association between WM microstructure and clinical symptoms, as measured by self-reported levels of social anxiety (z-SA) and intensity of FNE. Both analyses revealed that higher levels of z-SA and FNE were significantly associated with higher FA values and lower MD and RD values in the left and right SLF. These significant findings will be discussed more in depth in the following paragraphs. We did not find any significant correlations between levels of social anxiety or FNE and WM microstructure in the bilateral UF or ILF.

Voxelwise TOI analysis

Significant associations are summarized in Table 2 and illustrated in Figure 2. A cluster in the left SLF was significantly positively associated with levels of social anxiety and FNE (b = 0.147, p = 0.006 and b = 0.039, p = 0.002 resp.). In addition, a cluster in the right SLF was significantly positively associated with levels of FNE (b = 0.027, p = 0.04). In both clusters, these findings were coupled with significant negative associations between the level of clinical symptoms and MD and RD. AD was not significantly associated with clinical symptoms.

Table 2 Significant associations between measures of SA and voxelwise TOI analyses of fractional anisotropy in the SLF; post-hoc analyses of additional WM parameters within the clusters.

Clinical measure	Side	WM parameter	Voxels (mm^3)	Peak MNI coordinates			b	p
				x	y	z		
z-SA	L	FA	207	-32	-39	29	0.147	.006
		AD					0.071	.37
		MD					-0.012	.03
		RD					-0.076	< .001
FNE	L	FA	178	-33	-38	29	0.039	.002
		AD					0.017	.49
		MD					-0.004	.01
		RD					-0.021	< .001
FNE	R	FA	51	34	-30	32	0.027	.04
		AD					0.013	.50
		MD					-0.023	< .001
		RD					-0.023	< .001

Threshold-free cluster enhancement (TFCE) and family-wise error (FWE) corrected at p-values < 0.05. ß-values and p-values represent the outcome of the analyses on mean values of white matter integrity over all voxels. z-SA: social anxiety (z-score); FNE: fear of negative evaluation; FA: fractional anisotropy; AD: axial diffusivity; MD: mean diffusivity; RD: radial diffusivity; L: left; R: right.

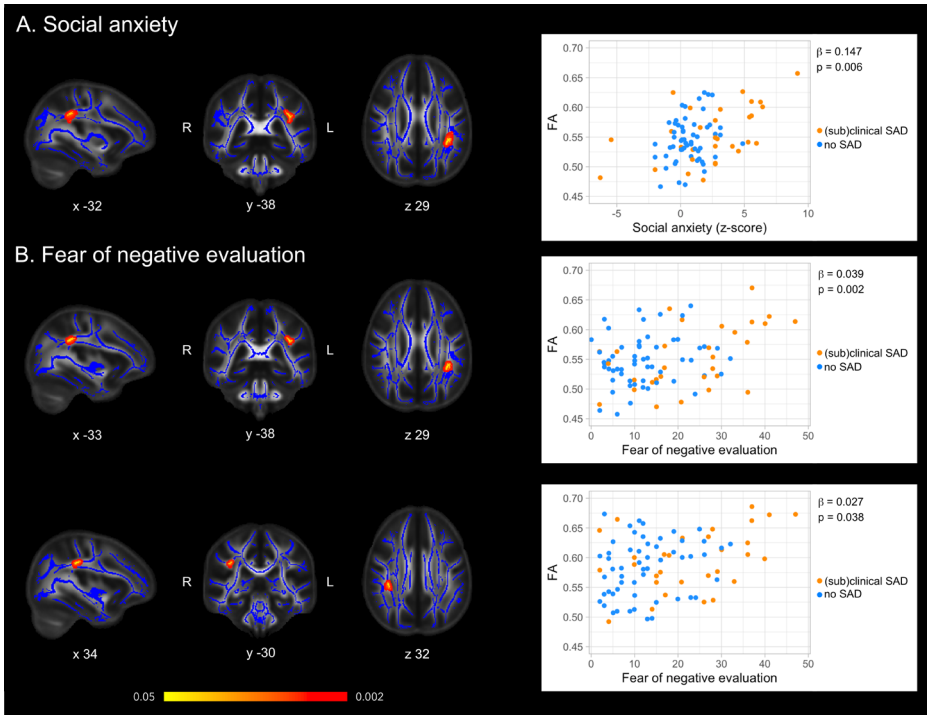

Figure 2 Significant clusters from voxelwise TOI analyses of fractional anisotropy in the superior longitudinal fasciculus. Sagittal, coronal and axial sections of the WM skeleton (blue), with subregions of the superior longitudinal fasciculus (SLF) showing significant associations of fractional anisotropy (FA) with levels of A) social anxiety (z-score) and B) fear of negative evaluation within families genetically enriched for social anxiety disorder (SAD) ($p < 0.05$, threshold-free cluster enhancement (TFCE) and family-wise error (FWE) corrected (yellow/orange)). The color bar indicates p-values.

Average TOI analysis

For all TOIs and all four parameters of WM microstructure, associations with clinical symptoms can be found in Table 3. In accordance with findings from the voxelwise TOI analyses, mean FA in the left SLF demonstrated a significant positive association with levels of self-reported social anxiety (b = 0.002, p = 0.03) and a near-significant association with levels of FNE (b = 3.67E-04, p = 0.06). In addition, mean FA in the right SLF showed a significant positive association with levels of intensity of FNE (b = 3.58E-04, p = 0.04). This finding was coupled with a significant negative association with mean RD values (b = -4.39E-07, p = 0.04) and a marginally significant, negative association with mean MD values (b = -3.15E-07, p = 0.09).

Heritability

Per TOI, heritability of every WM parameter was estimated over its average value. All results displayed at least moderate heritability (0.2 – 0.4), extending to very high heritability (0.9 – 1.0) for some WM parameters [91]. Results are summarized in Table 3.

Table 3 Associations between measures of SA and average values of white matter parameters in tracts of interest.

TOI	Side	WM parameter	Effect of social anxiety (z-score)			Effect of FNE			Heritability estimate	
			β	SE	p	β	SE	p	h^2	SE
ILF	L	FA	0.001	0.001	.58	3.44E-04	2.18E-04	.11	0.30	0.02
		AD	-4.46E-07	1.98E-06	.82	-1.37E-07	4.21E-07	.74	0.99	0.48
		MD	-9.58E-07	1.52E-06	.53	-3.38E-07	3.25E-07	.30	0.90	0.13
		RD	-1.20E-06	1.45E-06	.41	-4.17E-07	3.11E-07	.18	0.66	0.34
	R	FA	0.001	0.001	.28	1.89E-04	1.77E-04	.29	0.41	0.09
		AD	-3.46E-07	1.29E-06	.79	-1.15E-07	2.61E-07	.66	0.87	0.07
		MD	-1.09E-06	9.70E-07	.26	-2.57E-07	1.95E-07	.19	0.79	0.05
		RD	-1.35E-06	1.05E-06	.20	-2.66E-07	2.19E-07	.23	0.57	0.00
SLF	L	FA	0.002	0.001	.03	3.67E-04	1.92E-04	.06	0.41	0.05
		AD	1.15E-06	1.33E-06	.39	2.76E-08	2.75E-07	.92	0.73	0.21
		MD	-7.33E-07	1.13E-06	.51	-3.05E-07	2.34E-07	.19	0.70	0.01
		RD	-1.68E-06	1.21E-06	.17	-4.57E-07	2.55E-07	.07	0.59	0.03
	R	FA	0.001	0.001	.07	3.58E-04	1.76E-04	.04	0.31	0.02
		AD	1.21E-07	1.14E-06	.92	2.03E-08	2.26E-07	.93	0.84	0.05
		MD	-1.02E-06	9.14E-07	.27	-3.15E-07	1.84E-07	.09	0.78	0.05
		RD	-1.56E-06	1.04E-06	.13	-4.39E-07	2.16E-07	.04	0.58	0.04
UF	L	FA	0	0.001	.79	2.68E-04	3.19E-04	.40	0.37	0.05
		AD	1.16E-06	2.14E-06	.59	-1.43E-07	4.67E-07	.76	0.53	0.00
		MD	2.66E-07	1.56E-06	.86	-2.84E-07	3.38E-07	.40	0.51	0.01
		RD	-5.01E-08	1.68E-06	.98	-3.58E-07	3.59E-07	.32	0.51	0.10
	R	FA	0	0.001	.67	1.69E-04	2.48E-04	.50	0.61	0.02
		AD	1.05E-06	1.74E-06	.55	2.69E-07	3.77E-07	.48	0.26	0.01
		MD	-1.53E-07	9.36E-07	.87	-6.65E-09	1.91E-07	.97	0.73	0.01
		RD	-4.98E-07	1.11E-06	.65	-1.12E-07	2.27E-07	.62	0.72	0.14

TOI: tract of interest; WM: white matter; ILF: inferior longitudinal fasciculus; SLF: superior longitudinal fasciculus; UF: uncinate fasciculus; L: left; R: right; FA: fractional anisotropy; AD: axial diffusivity; MD: mean diffusivity; RD: radial diffusivity; FNE: fear of negative evaluation; SE: standard error; h^2: heritability estimate.

Discussion

In the present study we investigated whether characteristics of WM microstructure could be candidate endophenotypes of SAD. To our knowledge, this is the first comprehensive family study on WM microstructure in SAD, which enabled us to specifically examine co-segregation of WM characteristics in families of probands, as affected and non-affected family members have participated in this study (Bas-Hoogendam et al., 2018a). As recently stated by Glahn *et al.* [40], a multiplex, multigenerational family design like the LFLSAD is particularly powerful to investigate candidate endophenotypes as "[..] Reduced environmental variation among family members can reduce noise, improving statistical power to observe genotype-phenotype associations. [..] Designs that require multiple affected individuals in a family may result in a more severe phenotypic profile and a different underlying genetic architecture as compared to simplex families. [..] Family selection also impacts the distribution of phenotypes among unaffected family members, with members of multiplex families generally having greater endophenotype impairment than simplex family members."

In the present work, we focused on two endophenotype criteria, namely co-segregation of WM characteristics with social anxiety within participating families and estimation of heritability of these WM characteristics. Voxelwise and average tracts of interest (TOI) analyses were used to examine associations between measures of self-reported social anxiety and WM characteristics in the UF, SLF and ILF. For all three TOIs, heritability of WM characteristics was estimated.

Our analyses revealed that increased FA in the left and right SLF co-segregated with social anxiety within families enriched for SAD. These findings were coupled with decreased MD and RD and were consistent across both TOI analyses. The voxelwise results suggest that significant clusters are located in the SLF II. Furthermore, and in line with previous literature, all WM characteristics were estimated to be at least moderately heritable [50, 92].

The SLF II is the major part of the SLF and is mostly concerned with visuospatial attention and processing. Structurally it connects the caudal part of the inferior parietal lobule (IPL) and intraparietal sulcus with the posterior part of the prefrontal cortices. Functionally, the SLF II is thought to connect the parietal part of the ventral attention network with the prefrontal component of the dorsal attention network and is involved in the default mode network (DMN) [23, 24, 93-98].

Interestingly, previous studies that reported decreased FA and increased RD in the SLF described clusters in a different subpart of the SLF, namely SLF III, in patients with SAD compared to healthy controls (see Supplementary Table 1a and 1b; Tukel et al. [16], Qiu et al. [17], Baur et al. [21]. These findings were replicated in a meta-analysis using these three studies [12]. It should be noted that the SLF III differs from the SLF II as it extends from the supramarginal gyrus to the ventral premotor regions and is thought, among others, to be involved in language processing Schmahmann et al. [23], [24, 94]. In addition, the studies mentioned above had a different study design: they examined WM in SAD patients versus healthy controls in a case-control design, whilst we investigated WM microstructure in families

genetically enriched for SAD using a unique family study design. To the best of our knowledge, only one other study examining WM in SAD, using a case-control design and tractography analyses, reported increased FA [19]. In this study, the FA-increase was located in fibers passing through the genu of the corpus callosum.

Current literature suggests that increased FA coupled with decreased MD and RD and unchanged AD could imply dense axonal packaging or increased myelination [69, 99-101]. It should be noted that increased FA does not necessarily mean a better connection of the WM tract involved; instead, this could be suggestive of a compensatory mechanism, due to reduced crossing WM fibers or a more coherent alignment of fibers in the SLF II [99, 102, 103].

Our findings might seem contradictory to the neurofunctional model of the socially anxious brain described by Bruhl et al. [11], which proposed that decreased structural connectivity of, among others, the SLF could contribute to decoupling of hyperactive parietal and medial occipital brain regions from other networks involved in emotion regulation such as amygdala, limbic, salience and ventral attention networks. However, this subset of the model was based on the three DTI studies described above [16, 17, 21] and might yet be partly conceptual.

As recently reviewed by Bas-Hoogendam et al. [104], neuroimaging studies in SAD have reported multimodal changes in the brain. For example, changes in functional connectivity of the DMN have been reported. The DMN is thought to be involved in, among others, social referencing [15, 105]. In addition, cortical thickness and surface area of the IPL are positively associated with SAD [45]. Also, heightened activity in the medial temporal gyrus, superior temporal gyrus, and superior temporal sulcus during unintentional social norm processing is associated with SA [46] and a recent fMRI study by Kim et al. [106] reported heightened processing and prolonged attention during social threats in the IPL and the supramarginal gyrus. As the SLF II connects the IPL to the middle and superior frontal gyri, these results are relevant for the interpretation of our present findings.

We propose a few hypotheses for our findings, but realize that the current literature is not yet clear about the differentiation of subsets of the SLF and FA, and their involvement in SAD. First, the SLF II might be involved in the DMN as it connects different hubs of this network, and changes in the DMN have been reported in patients with SAD [15]. Second, the SLF II might be involved in abnormal visual processing as this tract is associated with posterior temporal parts and the attention network, and visual biases have been reported in SAD. Finally, FA is known to be decreased when strong fibers in multiple directions are present (e.g. in a crossing fiber area). If myelination of one fiber bundle in one of these directions is decreased, FA could be increased. Therefore, as our significant findings are in an area with a high amount of crossing fibers, we cautiously propose that increased social anxiety could be associated with lower myelination in one fiber bundle in a crossing fiber area.

Limitations and recommendations for future studies

Although this study is the first comprehensive two-generation family neuroimaging study on SAD, thus enabling investigation of WM microstructure as potential endophenotype of SAD, the findings of this study should be interpreted in light of its limitations. First, some participants have mental comorbid disorders, which thus might have influenced our results. However, as comorbidity is high in the clinical population of SAD patients [3-6], we deem our cohort as a representative sample. In addition, results of sensitivity analyses, in which we excluded participants with comorbid mental disorders, were in line with the main results. In addition, we would like to mention that although we used a continuous scale to analyze social anxiety rather than a dichotomous SAD versus non-SAD approach, we recognize our findings might not be SAD specific as changes in the SLF have also been reported in other mental emotional disorders, for example in a transdiagnostic meta-analysis of emotional disorders [12]. We therefore recommend future studies to consider transdiagnostic approaches, for example using the Research Domain Criteria framework [107].

Second, microstructure of WM tracts has been examined both in voxelwise and average TOI analyses to allow for interpretation in the light of the current literature whilst also being able to detect subtle changes in WM tracts. As we did not use tractography to analyze the DTI data, a method which is able to trace anatomical connections of WM between several brain regions and thus examine crossing fibers and different subsets of the SLF, we cannot investigate the idea that increased FA is a result of decreased myelination in one fiber bundle in a crossing fiber area. In addition, no post-hoc correction for the number of TOIs (n = 3, bilateral) has been applied thus results should be interpreted carefully. Also, analyses were done in the WM skeleton (and in TOIs), limiting it to the core of major WM tracts. As a result, more peripheral WM parameters in smaller tracts were not investigated. Therefore, future analyses should consider including tractography to investigate crossing fibers and distinguish between the different subsets of the SLF and their involvement in SAD. Also, we have only corrected linearly for age whilst the development of WM is known to peak at 28 years, followed by a slow decline [108]. In addition, the genetic data for GWAS analyses are not yet available, thus our findings cannot be linked to genetic variation yet. Finally, due to the lack of healthy control families without SAD, we could not examine the second part of the fourth endophenotype criterium (nonaffected family members show other levels of the endophenotype compared to the general population). As endophenotypes are thought to be present before the development of clinical symptoms, they should thus be measurable in unaffected family members and differ from healthy control families. This could not be investigated in the present study. In addition, as a cross-sectional design has been used, we could not examine the second endophenotype criterium (state-independency). Therefore, to further examine its potential role as an endophenotype, we advise future studies to consider including control families to compare changes in the SLF in nonaffected family members to SLF microstructure in healthy control families, and to consider a longitudinal design to study trait-stability.

Conclusion

The findings of the present work confirmed our hypothesis that altered white matter microstructure could be a candidate endophenotype of SAD. However, contradictory to our hypothesis of decreased FA, we found that increased FA in the SLF II co-segregated with SA within families genetically enriched for SAD. This was coupled with decreased RD and MD. Furthermore, all white matter characteristics were estimated to be at least moderately heritable, thus supporting the heritability criterion for endophenotypes. These findings might further elucidate the genetic susceptibility to SAD and improve our understanding of the overall etiology.

Supplemental Methods

Ethics

Every participant received €75 for participation in the LFLSAD (duration whole test procedure, including breaks: 8 hours) [44] and travel expenses were reimbursed. Furthermore, participants were provided with lunch/dinner, snacks and drinks during their visit to the lab. Confidentiality of the research data was maintained by the use of a unique research ID number for each participant.

Questionnaires

To estimate cognitive ability, we used the similarities (verbal comprehension) and block design (perceptual reasoning) subtests of the Wechsler Adult Intelligence Scale IV (WAIS-IV) [109] or Wechsler Intelligence Scale for Children III (WISC-III) [110].

Statistics

Differences in the presence of other psychopathology between (sub)clinical SAD and non-affected family members were assessed by the chi-square test in IBM SPSS Statistics for Windows [111] (10 tests, Bonferroni-corrected p-value = 0.005). Results can be found in Supplemental Table 2.

Reference values for z-scores on questionnaires

The following references were used (mean ± SD): LSAS-SR: 13.5 ± 12.7 [59]; SAS-A: 34.7 ± 2.3 [112]; BDI-II: 10.6 ± 10.9 [113]; CDI: 8.9 ± 5.4, unpublished data from the study by [112].

DTI-preprocessing

Prior to the MRI scan, all participants were informed about the MRI safety procedures and they were told that they could refrain from continuing the experiment at any time. Children and adolescents were familiarized with the MRI scanner using a mock scanner [114].

DWI data were converted to DICOM file format using dcm2niix [115].

Association between SAD diagnosis and parameters of WM integrity in TOI analyses

We examined the relationship between WM integrity and a diagnosis of (sub)clinical SAD in both voxelwise TOI analyses (using NINGA) and average TOI analyses in a similar way to the dimensional TOI analyses. As we assumed the same endophenotype to be reflected in both clinical and subclinical cases, (sub)clinical SAD was modelled as the independent variable. Covariate inference was incorporated in the model to account for nuisance kinship, gender and age. In order to obtain a reliable estimate of the main effect of (sub)clinical SAD, an interaction term assessing (sub)clinical SAD-by-age was also included in the model. Because data on the presence of subclinical SAD were, due to technical reasons, lost for six family members, data from these participants could not be used for this analysis (remaining sample: n = 88). Again, additional WM parameters were examined for significant FA clusters only.

Voxelwise analysis of whole WM skeleton

For reasons of completeness, we also explored voxelwise co-segregation of social anxiety with WM integrity in the white matter tracts in the skeleton using NINGA. Individual levels of self-reported social anxiety (z-SA and FNE) were modelled as independent variables and voxelwise FA values as the dependent variable. Covariate inference was incorporated in the model to account for nuisance kinship, gender and age. We used Threshold-Free Cluster Enhancement (TFCE) statistics to define significant clusters, and permutation testing to provide FWE-corrected p-values at a conventional threshold of a = 0.05 to correct for multiple comparisons. Additional parameters of WM integrity, being RD, MD and AD, were examined for significant clusters only by extracting and binarizing the significant FA cluster from the previous analysis. This mask was then used to comprise only the relevant voxels in individual skeletons of AD, MD and RD. Next, individual levels of self-reported social anxiety symptoms (z-SA and FNE) were modelled as independent variables and AD, MD or RD in the relevant cluster as the dependent variable. Again, covariate inference was incorporated to account for nuisance kinship, gender and age.

Supplemental Results

Sample characteristics after quality checking and data availability

The sample for the present analyses consisted of data of 110 participants from eight families (56 males (50.9 %), mean number of participating family members per family: 13.8, range 5 – 28). These family members were, according to the design, divided over two generations (generation 1: n = 51, 24 males; age (mean ± SD, range) 46.5 ± 6.7 years, 34.3 – 61.5 years; generation 2: n = 59, 32 males, age 18.1 ± 6.0 years, 9.0 – 32.2 years) who differed significantly in age ($\beta = -30.3$, $p < 0.001$), but not in male/female ratio ($\chi^2 = 0.56$, $p = 0.57$). After pre-processing, data from n = 94 participants was available for further analysis, as for two subjects BET was unable to adequately extract non-brain tissue images and an additional twelve subjects had to be excluded due to excessive head motion (defined as relative head motion with respect to the previous volume > 2.5 mm).

Association between (sub)clinical SAD diagnosis and parameters of WM integrity in TOI analyses

There were no significant correlations between a diagnosis of (sub)clinical SAD and measures of diffusivity in any of the three TOIs (see Supplemental Table 3 for results of average TOI analyses).

Voxelwise analysis of whole WM skeleton

No significant clusters were found. However, when applying a liberal threshold of FWE-corrected $p < 0.1$, levels of self-reported social anxiety scores showed a near-significant positive association with one cluster of FA in the left SLF (FWE corrected TFCE value $p = 0.093$, $\beta = 0.176$). This was coupled with a negative association with RD and no significant associations of AD or MD. See Supplemental Table 4 for more details.

Sensitivity analyses

Although SAD is associated with high rates of comorbidity [5, 116], we performed a sensitivity analysis in order to examine the effects (associations) of social anxiety disorder independent from comorbidity (sensitivity analysis 1), by excluding participants with (comorbid) psychopathology. Note however, that the results of this analysis may be biased as the majority of the probands, on which the selection of the families was based, were excluded.

In the remaining sample (n = 50, SAD patients: n = 11; HC: n = 39), in the voxelwise TOI analysis we found a correlation between levels of social anxiety (z-SA) and FA in the right ILF (see Supplemental Table 5). In the average TOI analysis, near-significant positive associations with mean FA values in bilateral ILF and SLF and levels of social anxiety (z-SA) were found. This was accompanied by negative associations with levels of social anxiety and mean RD and MD values in those regions. There was no effect of FNE (see Supplemental Table 6).

When the level of depressive symptoms (z-score) was added as a covariate to the model (sensitivity analysis 2), in the voxelwise TOI analyses both levels of FNE and SA were significantly associated with a cluster of FA in the left SLF (see Supplemental Table 5). In the average TOI analyses, no association maintained conventional p-values below 0.05, although mean FA values in the left SLF reached a near-significant trend association with levels of social anxiety (b = 0.002, p = 0.08) (see Supplemental Table 7). Because of these findings, the effect of levels of depressive symptoms (z-score) on white matter integrity in all TOIs was examined as well (again corrected for age and gender; see Supplemental Table 7). No significant associations between the level of depressive symptoms and WM indices were found.

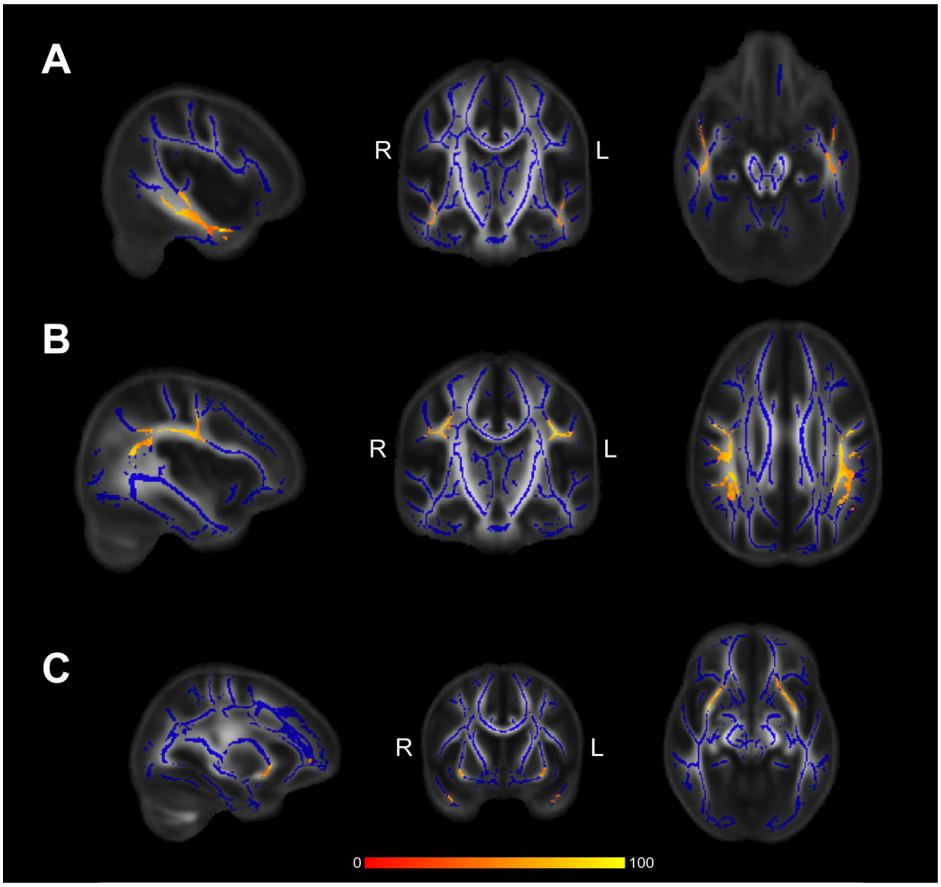

Supplemental Figure 1 Tracts (TOIs) used in analyses. Sagittal, coronal and axial sections of the WM skeleton (blue), with mean FA for tractwise analyses of resp. A) inferior longitudinal fasciculus (ILF), B) superior longitudinal fasciculus (SLF) and C) uncinate fasciculus (UF) (TOIs depicted in yellow/orange). The colour bar represents the probability of voxels belonging to the respective tract.

Supplemental Table 1a Overview of previous literature, descriptive information.

Author & journal	Contrast	Patients	Age (years)	LSAS	Depressive symptoms	Illness (months)	HC	Age (years)	LSAS	Depressive symptoms
Phan et al. [18]	SAD vs. HC	15 M / 15 F	27.2 ± 7.8	76.6 ± 17.3	BDI = 10.7 ± 6.5	n.a.	10 M / 20 F	29.9 ± 8.1	13.4 ± 11.3	BDI = 1.8 ± 2.4
Baur et al. [21] [a]	SAD vs. HC	18 M / 7 F	32.0 ± 10.4	66.0 ± 23.0	BDI = 15 ± 10.8	192	18 M / 7 F	32.0 ± 10.1	n.a.	n.a.
Liao et al. [19] [b]	SAD vs. HC	12 M / 6 F	22.7 ± 3.7	54.4 ± 12.0	HAM-D = 7.3 ± 6.2	49.2	13 M / 5 F	21.9 ± 3.7	19.1 ± 7.9	HAM-D = 1.0 ± 1.6
Baur et al. [20] [a]	SAD vs. HC	18 M / 7 F	31.6 ± 10.4	66.0 ± 23.0	BDI = 15 ± 10.8	192	18 M / 7 F	32.3 ± 10.1	n.a.	n.a.
Qiu et al. [17] [b]	SAD vs. HC	12 M / 6 F	22.7 ± 3.9	54.1 ± 11.9	n.a.	49.2	12 M / 6 F	21.8 ± 3.9	19.5 ± 8.5	n.a.
Jenkins et al. [12]	Within SAD	45 M / 28 F	n.a.	n.a.	n.a.	n.a.	n.a.	n.a.	n.a.	n.a.
Tukel et al. [16]	SAD vs. HC	11 M / 11 F	27.7 ± 6.6	73.9 ± 28.5	HAM-D = 4.1 ± 4.5	14.4	11 M / 11 F	28.7 ± 6.6	n.a.	n.a.

Age and questionnaire data are reported as mean ± SD. [a] Study results seem derived from the same sample. [b] Study results seem derived from the same sample. M: male; F: female; SAD: social anxiety disorder; HC: healty control participants; BDI: Beck Depression Inventory; HAM-D: Hamilton Depression Rating Scale; n.a: no data available.

Supplemental Table 1b Overview of previous literature, findings.

	Main analysis method	WM alterations	CST	IFOF		ILF		SLF		UF		AF	
				L	R	L	R	L	R	L	R	L	R
[18]	Voxelwise	FA	ø	ø	ø	ø	ø	ø	ø	ø	↓		ø
[21]	Voxelwise	FA	ø	ø	ø	ø	ø	↓	ø	↓	ø		ø
		RD ROI								ø	ø		
		AD ROI								ø	ø		
		FA association with trait anxiety (SAD only)						ø	ø	↓	↓		
		AD association with trait anxiety						ø	ø	↓	ø		
		FA association with social anxiety						ø	ø	ø	ø		
[19]	Tractography	FA ROI											↑
		Fiber tracking density											↑
		FA association with social anxiety											
[20]	Tractography	FA	ø	ø	ø					↓	ø		
		Volume	ø	ø	ø					↓	↓		
		FA association with social anxiety								↓	ø		
		FA association with trait anxiety								ø	ø		
[17]	Voxelwise	FA	ø	ø	ø	ø	ø	↓	ø	↓	ø		ø
		MD	ø	↑	↑	ø	ø	↑	↑	ø	ø		ø
		FA association with social anxiety		ø	ø			↓	ø	↓	ø		
		MD association with social anxiety		ø	ø			↑	ø	ø	ø		
[12]	Voxelwise meta-analysis	FA	↓	ø	ø	ø	ø	↓	ø	↓	↓		ø
		Association with social anxiety											

Supplemental Table 1b Overview of previous literature, findings. (continued)

[16]	Voxelwise	FA	ø	ø	ø	ø	↓	ø	↓	ø	ø		ø		
		MD ROI					ø		ø						
		AD ROI					↓		↓						
		RD ROI					↑		↑						
		FA association with social anxiety					ø		↓						
		MD association with social anxiety					ø		ø						
		AD association with social anxiety					ø		ø						
		RD association with social anxiety					ø		ø						

FA: fractional anisotropy; RD: radial diffusivity; AD: axial diffusivity; MD: mean diffusivity; ROI: region of interest; ↓: decreased in SAD; ↑: increased in SAD; ø: no difference between SAD and HCs; CST: corticospinal tract; IFOF: inferior fronto-occipital fasciculus; ILF: inferior longitudinal fasciculus; SLF: superior longitudinal fasciculus; UF: uncinate fasciculus; AF: arcuate fasciculus; L: left; R: right. Empty cells indicate no data was available.

Supplemental Table 2 Additional diagnostic information of participants within the LFLSAD.

Diagnostic information (n)	(Sub)clinical SAD (n = 31)	No SAD (n = 57)	Statistical analysis
Depressive episode – present	1	1	$c^2 = 0.23$, p = .62
Depressive episode – past	10	9	$c^2 = 3.93$, p = .05*
Dysthymia – present	2	0	$c^2 = 4.03$, p = .05*
Dysthymia – past	0	1	$c^2 = 0.46$, p = .50
Panic disorder – lifetime	4	2	$c^2 = 3.14$, p = .08
Agoraphobia – present	2	1	$c^2 = 1.51$, p = .22
Agoraphobia – past	0	2	$c^2 = 1.04$, p = .31
Separation anxiety	0	1	$c^2 = 0.83$, p = .36
Specific phobia	2	3	$c^2 = 0.08$, p = .78
Generalized anxiety disorder	1	0	$c^2 = 1.99$, p = .16
Obsessive-compulsive disorder	1	0	$c^2 = 1.99$, p = .16
Alcohol dependency present	0	1	$c^2 = 0.52$, p = .47
Alcohol dependency lifetime	0	3	$c^2 = 1.59$, p = .21

SAD: social anxiety disorder.* significant at uncorrected p-value of 0.05.

Supplemental Table 3 Effects of (sub)clinical SAD on average white matter integrity per tract (TOI).

TOI	Side	WM parameter	Effect of (sub)clinical SAD		
			β	SE	p
ILF	L	FA	-0.002	0.004	.55
		AD	9.56E-07	6.24E-06	.88
		MD	4.50E-06	4.88E-06	.36
		RD	5.05E-06	5.48E-06	.36
	R	FA	0.003	0.004	.54
		AD	1.48E-06	6.24E-06	.81
		MD	5.42E-07	4.81E-06	.91
		RD	5.42E-08	5.29E-06	.99
SLF	L	FA	0.001	0.004	.74
		AD	3.28E-06	5.66E-06	.56
		MD	1.72E-06	4.92E-06	.73
		RD	8.91E-08	5.71E-06	.99
	R	FA	0.002	0.004	.61
		AD	-8.07E-07	5.57E-06	.88
		MD	8.12E-08	4.59E-06	.99
		RD	-8.63E-07	5.30E-06	.87
UF	L	FA	-0.005	0.006	.47
		AD	-9.42E-06	7.92E-06	.23
		MD	-6.96E-07	5.37E-06	.90
		RD	3.53E-06	6.73E-06	.60
	R	FA	-0.002	0.006	.79
		AD	1.77E-07	8.47E-06	.98
		MD	8.30E-07	4.65E-06	.86
		RD	1.91E-06	5.62E-06	.73

TOI: tract of interest; WM: white matter parameter; ILF: inferior longitudinal fasciculus; SLF: superior longitudinal fasciculus; UF: uncinate fasciculus; FA: fractional anisotropy; AD: axial diffusivity; MD: mean diffusivity; RD: radial diffusivity; L: left; R: right; SE: standard error.

Supplemental Table 4 Associations between measures of SA and exploratory voxelwise analyses of fractional anisotropy over the whole WM skeleton and results of post-hoc analyses of additional parameters.

Clinical measure	Anatomical region	WM parameter	Voxels (mm^3)	Peak MNI coordinates				
				x	y	z	b	p
z-SA	SLF (L)	FA	56	-33	-37	30	0.176	.093
		AD					0.107	.85
		MD					0.002	.12
		RD					-0.090	.001

Threshold-free cluster enhancement (TFCE) and family-wise error (FWE) corrected at threshold of $p < 0.1$. ß-values and p-values represent mean values of white matter integrity over all voxels. z-SA: social anxiety (z-score); L: left; WM: white matter parameter; FA: fractional anisotropy; AD: axial diffusivity; MD: mean diffusivity; RD: radial diffusivity.

Supplemental Table 5 Significant results of sensitivity analyses 1 and 2 in voxelwise TOI analyses of fractional anisotropy in the superior longitudinal fasciculus.

Sensitivity analysis	Clinical measure	ROI	Side	Voxels (mm^3)	Peak MNI coordinates				
					x	y	z	b	p
1	z-SA	ILF	R	26	38	-47	-5	0.268	.027
2	FNE	SLF	L	62	-33	-37	29	0.002	.025
2	z-SA	SLF	L	154	-33	-37	30	0.009	.016

Threshold-free cluster enhancement (TFCE) and family-wise error (FWE) corrected at $p < 0.05$. Sensitivity analysis 1: model without participants with comorbid psychopathology (e.g. patients with a single SAD diagnosis vs. healthy control participants). Sensitivity analysis 2: model with levels of depression added as additional covariate. FNE: fear of negative evaluation; z-SA: social anxiety (z-score); SLF: superior longitudinal fasciculus; ILF: inferior longitudinal fasciculus; L: left; R: right.

Supplemental Table 6 Results of sensitivity analysis 1: sample consisting of participants without (comorbid) psychopathology. Effects of levels of social anxiety and FNE on average values of white matter integrity per TOI.

			Effect of social anxiety (z-score)			Effect of FNE		
			β	SE	p	β	SE	p
ILF	L	FA	0.003	0.002	.08	3.78E-04	2.96E-04	.20
		AD	1.21E-06	2.09E-06	.56	2.45E-07	4.11E-07	.55
		MD	-2.82E-06	1.60E-06	.08	-3.48E-07	3.21E-07	.28
		RD	-4.06E-06	1.92E-06	.03*	-4.49E-07	3.81E-07	.24
	R	FA	0.003	0.002	.09	3.04E-04	3.36E-04	.37
		AD	5.93E-07	2.29E-06	.80	-1.82E-07	4.40E-07	.68
		MD	-2.67E-06	1.60E-06	.10	-4.14E-07	3.15E-07	.19
		RD	-3.84E-06	2.01E-06	.06	-3.74E-07	3.98E-07	.35
SLF	L	FA	0.003	0.002	.07	1.45E-04	3.65E-04	.69
		AD	1.50E-06	2.00E-06	.45	1.32E-07	3.88E-07	.73
		MD	-2.79E-06	1.79E-06	.12	-3.38E-07	3.54E-07	.34
		RD	-4.25E-06	2.26E-06	.06	-4.28E-07	4.46E-07	.34
	R	FA	0.004	0.002	.05	1.69E-04	3.62E-04	.64
		AD	3.50E-07	2.07E-06	.87	-8.86E-09	4.01E-07	.98
		MD	-3.24E-06	1.66E-06	.05	-4.44E-07	3.34E-07	.18
		RD	-4.44E-06	2.15E-06	.03*	-5.07E-07	4.23E-07	.23
UF	L	FA	0.002	0.002	.40	-1.91E-04	4.18E-04	.65
		AD	-5.71E-07	2.99E-06	.85	-3.08E-07	5.66E-07	.59
		MD	-1.63E-06	1.67E-06	.33	-1.77E-07	3.28E-07	.59
		RD	-2.04E-06	2.04E-06	.32	-1.29E-07	4.03E-07	.75
	R	FA	0.000	0.002	.90	-4.47E-04	3.86E-04	.25
		AD	2.45E-06	3.01E-06	.42	1.90E-08	5.80E-07	.97
		MD	2.82E-07	1.64E-06	.86	3.29E-07	3.10E-07	.29
		RD	8.77E-07	1.69E-06	.60	4.49E-07	3.32E-07	.18

ILF: inferior longitudinal fasciculus; SLF: superior longitudinal fasciculus; UF: uncinate fasciculus; FNE: fear of negative evaluation; FA: fractional anisotropy; AD: axial diffusivity; MD: mean diffusivity; RD: radial diffusivity; L: left; R: right; SE: standard error;* significant at p-value of 0.05.

Supplemental Table 7 Results of sensitivity analysis 2: effects of levels of depression on the effects of levels of social anxiety and FNE on average values of white matter integrity per TOI average values of white matter integrity per TOI.

β			Effect of social anxiety (z-score)			Effect of FNE			Effect of depression (z-score)		
			β	SE	p	β	SE	p	β	SE	p
ILF	L	FA	2.97E-04	0.001	.79	4.29E-04	2.74E-04	.12	0.002	0.003	.46
		AD	3.23E-07	2.17E-06	.88	1.46E-07	5.29E-07	.78	-5.12E-06	5.67E-06	.37
		MD	-5.05E-07	1.67E-06	.76	-2.71E-07	4.09E-07	.51	-3.82E-06	4.38E-06	.38
		RD	-8.76E-07	1.59E-06	.58	-4.42E-07	3.92E-07	.26	-3.35E-06	4.19E-06	.42
	R	FA	8.49E-04	0.001	.35	2.25E-04	2.23E-04	.31	0.001	0.002	.61
		AD	-2.07E-07	1.42E-06	.88	-9.48E-08	3.28E-07	.77	-1.17E-06	3.66E-06	.75
		MD	-9.39E-07	1.07E-06	.38	-2.50E-07	2.45E-07	.31	-2.18E-06	2.78E-06	.43
		RD	-1.19E-06	1.16E-06	.30	-2.50E-07	2.76E-07	.36	-2.50E-06	3.04E-06	.41
SLF	L	FA	0.002	0.001	.08	3.58E-04	2.43E-04	.14	0.003	0.003	.20
		AD	1.67E-06	1.46E-06	.25	1.47E-07	3.45E-07	.67	-1.56E-06	3.84E-06	.68
		MD	-3.26E-07	1.24E-06	.79	-2.67E-07	2.94E-07	.36	-3.21E-06	3.23E-06	.32
		RD	-1.28E-06	1.33E-06	.33	-4.36E-07	3.21E-07	.17	-4.30E-06	3.50E-06	.22
	R	FA	0.001	0.001	.15	3.54E-04	2.21E-04	.11	0.003	0.002	.21
		AD	4.77E-07	1.25E-06	.70	1.70E-07	2.81E-07	.54	-1.81E-06	3.22E-06	.58
		MD	-5.68E-07	1.00E-06	.57	-2.32E-07	2.31E-07	.32	-3.74E-06	2.59E-06	.15
		RD	-1.04E-06	1.13E-06	.36	-3.57E-07	2.72E-07	.19	-4.77E-06	2.98E-06	.11
UF	L	FA	4.13E-04	0.002	.80	4.29E-04	3.99E-04	.28	0.000	0.004	.95
		AD	2.13E-06	2.34E-06	.36	4.91E-08	5.91E-07	.93	-3.79E-06	6.19E-06	.54
		MD	8.40E-07	1.72E-06	.63	-2.36E-07	4.26E-07	.58	-3.31E-06	4.52E-06	.46
		RD	-1.04E-06	1.13E-06	.36	-3.57E-07	2.72E-07	.19	-4.77E-06	2.98E-06	.11
	R	FA	9.79E-04	0.001	.45	4.18E-04	3.08E-04	.17	-0.002	0.003	.53
		AD	1.81E-06	1.92E-06	.35	6.26E-07	4.73E-07	.19	-2.74E-06	5.05E-06	.59
		MD	-2.32E-07	1.03E-06	.82	-2.85E-08	2.40E-07	.91	2.57E-07	2.69E-06	.92
		RD	-9.41E-07	1.22E-06	.44	-3.13E-07	2.83E-07	.27	1.87E-06	3.17E-06	.56

ILF: inferior longitudinal fasciculus; SLF: superior longitudinal fasciculus; UF: uncinate fasciculus; FNE: fear of negative evaluation; FA: fractional anisotropy; AD: axial diffusivity; MD: mean diffusivity; RD: radial diffusivity; L: left; R: right; SE: standard error

References

1. Bas-Hoogendam, J.M., et al., *Pathogenesis of social anxiety disorder*, in *The american psychiatric association publishing textbook of anxiety, trauma, and ocd-related disorders, third edition*, N. Simon, et al., Editors. 2020, American Psychiatric Association Publishing: Washington, DC.
2. American Psychiatric Association, *Diagnostic and statistical manual of mental disorders, fifth edition (dsm-5)*, ed. A.P. Association. 2013, Washington, DC: American Psychiatric Association Publishing.
3. Koyuncu, A., et al., *Comorbidity in social anxiety disorder: Diagnostic and therapeutic challenges.* Drugs Context, 2019. **8**: p. 212573.
4. Blanco, C., et al., *Predictors of persistence of social anxiety disorder: A national study.* J Psychiatr Res, 2011. **45**(12): p. 1557-63.
5. Grant, B.F., et al., *The epidemiology of social anxiety disorder in the united states: Results from the national epidemiologic survey on alcohol and related conditions.* J Clin Psychiatry, 2005. **66**(11): p. 1351-61.
6. Fehm, L., et al., *Size and burden of social phobia in europe.* Eur Neuropsychopharmacol, 2005. **15**(4): p. 453-62.
7. Beesdo-Baum, K., et al., *The natural course of social anxiety disorder among adolescents and young adults.* Acta Psychiatr Scand, 2012. **126**(6): p. 411-25.
8. Steinert, C., et al., *What do we know today about the prospective long-term course of social anxiety disorder? A systematic literature review.* J Anxiety Disord, 2013. **27**(7): p. 692-702.
9. Stein, M.B. and D.J. Stein, *Social anxiety disorder.* Lancet, 2008. **371**(9618): p. 1115-25.
10. Fox, A.S. and N.H. Kalin, *A translational neuroscience approach to understanding the development of social anxiety disorder and its pathophysiology.* Am J Psychiatry, 2014. **171**(11): p. 1162-73.
11. Bruhl, A.B., et al., *Neuroimaging in social anxiety disorder-a meta-analytic review resulting in a new neurofunctional model.* Neurosci Biobehav Rev, 2014. **47**: p. 260-80.
12. Jenkins, L.M., et al., *Shared white matter alterations across emotional disorders: A voxel-based meta-analysis of fractional anisotropy.* Neuroimage Clin, 2016. **12**: p. 1022-1034.
13. Etkin, A. and T.D. Wager, *Functional neuroimaging of anxiety: A meta-analysis of emotional processing in ptsd, social anxiety disorder, and specific phobia.* Am J Psychiatry, 2007. **164**(10): p. 1476-88.
14. Hahn, A., et al., *Reduced resting-state functional connectivity between amygdala and orbitofrontal cortex in social anxiety disorder.* Neuroimage, 2011. **56**(3): p. 881-9.
15. MacNamara, A., J. DiGangi, and K.L. Phan, *Aberrant spontaneous and task-dependent functional connections in the anxious brain.* Biol Psychiatry Cogn Neurosci Neuroimaging, 2016. **1**(3): p. 278-287.
16. Tukel, R., et al., *Evidence for alterations of the right inferior and superior longitudinal fasciculi in patients with social anxiety disorder.* Brain Res, 2017. **1662**: p. 16-22.
17. Qiu, C., et al., *Diffusion tensor imaging studies on chinese patients with social anxiety disorder.* Biomed Res Int, 2014. **2014**: p. 860658.
18. Phan, K.L., et al., *Preliminary evidence of white matter abnormality in the uncinate fasciculus in generalized social anxiety disorder.* Biol Psychiatry, 2009. **66**(7): p. 691-4.
19. Liao, W., et al., *Altered gray matter morphometry and resting-state functional and structural connectivity in social anxiety disorder.* Brain Res, 2011. **1388**: p. 167-77.
20. Baur, V., et al., *Evidence of frontotemporal structural hypoconnectivity in social anxiety disorder: A quantitative fiber tractography study.* Hum Brain Mapp, 2013. **34**(2): p. 437-46.
21. Baur, V., et al., *White matter alterations in social anxiety disorder.* J Psychiatr Res, 2011. **45**(10): p. 1366-72.
22. Von Der Heide, R.J., et al., *Dissecting the uncinate fasciculus: Disorders, controversies and a hypothesis.* Brain, 2013. **136**(Pt 6): p. 1692-707.
23. Schmahmann, J.D., et al., *Association fibre pathways of the brain: Parallel observations from diffusion spectrum imaging and autoradiography.* Brain, 2007. **130**(Pt 3): p. 630-53.
24. Schmahmann, J.D. and D.N. Pandya, *Fiber pathways of the brain*, in *Fiber pathways of the brain*. 2006. p. 409-414.
25. Catani, M., et al., *Occipito-temporal connections in the human brain.* Brain, 2003. **126**(9): p. 2093-107.
26. Maller, J.J., et al., *Revealing the hippocampal connectome through super-resolution 1150-direction diffusion mri.* Sci Rep, 2019. **9**(1): p. 2418.
27. Panesar, S.S., et al., *A quantitative tractography study into the connectivity, segmentation and laterality of the human inferior longitudinal fasciculus.* Front Neuroanat, 2018. **12**(47): p. 47.
28. Steiger, V.R., et al., *Pattern of structural brain changes in social anxiety disorder after cognitive behavioral group therapy: A longitudinal multimodal mri study.* Mol Psychiatry, 2017. **22**(8): p. 1164-1171.
29. Whitfield-Gabrieli, S., et al., *Brain connectomics predict response to treatment in social anxiety disorder.* Mol Psychiatry, 2016. **21**(5): p. 680-5.
30. Kim, M.J. and P.J. Whalen, *The structural integrity of an amygdala-prefrontal pathway predicts trait anxiety.* J Neurosci, 2009. **29**(37): p. 11614-8.
31. Kim, M.J., et al., *The inverse relationship between the*

microstructural variability of amygdala-prefrontal pathways and trait anxiety is moderated by sex. Front Syst Neurosci, 2016. **10**: p. 93.

32. Sylvester, C.M., et al., *Functional network dysfunction in anxiety and anxiety disorders.* Trends Neurosci, 2012. **35**(9): p. 527-35.
33. Peer, M., et al., *Evidence for functional networks within the human brain's white matter.* J Neurosci, 2017. **37**(27): p. 6394-6407.
34. Wong, Q.J.J. and R.M. Rapee, *The aetiology and maintenance of social anxiety disorder: A synthesis of complimentary theoretical models and formulation of a new integrated model.* J Affect Disord, 2016. **203**: p. 84-100.
35. Spence, S.H. and R.M. Rapee, *The etiology of social anxiety disorder: An evidence-based model.* Behav Res Ther, 2016. **86**: p. 50-67.
36. Scaini, S., R. Belotti, and A. Ogliari, *Genetic and environmental contributions to social anxiety across different ages: A meta-analytic approach to twin data.* J Anxiety Disord, 2014. **28**(7): p. 650-6.
37. Stein, M.B., et al., *Genetic risk variants for social anxiety.* Am J Med Genet B Neuropsychiatr Genet, 2017. **174**(2): p. 120-131.
38. Gottesman, II and T.D. Gould, *The endophenotype concept in psychiatry: Etymology and strategic intentions.* Am J Psychiatry, 2003. **160**(4): p. 636-45.
39. Lenzenweger, M.F., *Endophenotype, intermediate phenotype, biomarker: Definitions, concept comparisons, clarifications.* Depress Anxiety, 2013. **30**(3): p. 185-9.
40. Glahn, D.C., et al., *Rediscovering the value of families for psychiatric genetics research.* Mol Psychiatry, 2019. **24**(4): p. 523-535.
41. Roffman, J.L., *Endophenotype research in psychiatry-the grasshopper grows up.* JAMA Psychiatry, 2019.
42. Miller, G.A. and B. Rockstroh, *Endophenotypes in psychopathology research: Where do we stand?* Annu Rev Clin Psychol, 2013. **9**(1): p. 177-213.
43. Bas-Hoogendam, J.M., et al., *Neurobiological candidate endophenotypes of social anxiety disorder.* Neurosci Biobehav Rev, 2016. **71**: p. 362-378.
44. Bas-Hoogendam, J.M., et al., *The leiden family lab study on social anxiety disorder: A multiplex, multigenerational family study on neurocognitive endophenotypes.* Int J Methods Psychiatr Res, 2018. **27**(2): p. e1616.
45. Bas-Hoogendam, J.M., et al., *Subcortical brain volumes, cortical thickness and cortical surface area in families genetically enriched for social anxiety disorder - a multiplex multigenerational neuroimaging study.* EBioMedicine, 2018. **36**: p. 410-428.
46. Bas-Hoogendam, J.M., et al., *Altered neurobiological processing of unintentional social norm violations: A multiplex, multigenerational functional magnetic resonance imaging study on social anxiety endophenotypes.* Biol Psychiatry Cogn Neurosci Neuroimaging, 2019.
47. Bas-Hoogendam, J.M., et al., *Impaired neural habituation to neutral faces in families genetically enriched for social anxiety disorder.* Depress Anxiety, 2019. **36**(12): p. 1143-1153.
48. Bas-Hoogendam, J.M., et al., *P.491 social conditioning of neutral faces in families genetically enriched for social anxiety disorder.* European Neuropsychopharmacology, 2019. **29**: p. S345-S346.
49. Bas-Hoogendam, J.M., et al., *Amygdala hyperreactivity to faces conditioned with a social-evaluative meaning- a multiplex, multigenerational fmri study on social anxiety endophenotypes.* NeuroImage Clin, 2020. **26**: p. 102247.
50. Kochunov, P., et al., *Heritability of fractional anisotropy in human white matter: A comparison of human connectome project and enigma-dti data.* Neuroimage, 2015. **111**: p. 300-11.
51. Budisavljevic, S., et al., *Heritability of the limbic networks.* Soc Cogn Affect Neurosci, 2016. **11**(5): p. 746-57.
52. Smith, S.M., et al., *Tract-based spatial statistics: Voxelwise analysis of multi-subject diffusion data.* Neuroimage, 2006. **31**(4): p. 1487-505.
53. van der Werff, S.J., et al., *Widespread reductions of white matter integrity in patients with long-term remission of cushing's disease.* NeuroImage Clin, 2014. **4**: p. 659-67.
54. Aghajani, M., et al., *Altered white-matter architecture in treatment-naive adolescents with clinical depression.* Psychol Med, 2014. **44**(11): p. 2287-98.
55. Sheehan, D.V., et al., *The mini-international neuropsychiatric interview (m.I.N.I.): The development and validation of a structured diagnostic psychiatric interview for dsm-iv and icd-10.* J Clin Psychiatry, 1998. **59 Suppl 20**: p. 22-33;quiz 34-57.
56. Sheehan, D.V., et al., *Reliability and validity of the mini international neuropsychiatric interview for children and adolescents (mini-kid).* J Clin Psychiatry, 2010. **71**(3): p. 313-26.
57. van Vliet, I.M. and E. de Beurs, *[the mini-international neuropsychiatric interview. A brief structured diagnostic psychiatric interview for dsm-iv en icd-10 psychiatric disorders].* Tijdschr Psychiatr, 2007. **49**(6): p. 393-7.
58. Bauhuis, O., et al., *De introductie van een nederlandstalig instrument om dsm-iv-tr-diagnoses bij kinderen te stellen.* Kind & Adolescent Praktijk, 2013. **12**(1): p. 20-26.
59. Fresco, D.M., et al., *The liebowitz social anxiety scale: A comparison of the psychometric properties of self-report and clinician-administered formats.* Psychol Med, 2001. **31**(6): p. 1025-35.

60. Mennin, D.S., et al., *Screening for social anxiety disorder in the clinical setting: Using the liebowitz social anxiety scale.* Journal of Anxiety Disorders, 2002. **16**(6): p. 661-673.
61. La Greca, A.M. and N. Lopez, *Social anxiety among adolescents: Linkages with peer relations and friendships.* J Abnorm Child Psychol, 1998. **26**(2): p. 83-94.
62. Carleton, R.N., et al., *Brief fear of negative evaluation scale-revised.* Depress Anxiety, 2006. **23**(5): p. 297-303.
63. Leary, M.R., *A brief version of the fear of negative evaluation scale.* Pers Soc Psychol B, 2016. **9**(3): p. 371-375.
64. Spielberger, C.D., R.L. Gorsuch, and R.E. Lushene, *Stai manual for the state-trait anxiety inventory*. 1970, Palo Alto, CA: Consulting Psychologists Press.
65. Beck, A.T., R. Steer, and G. Brown, *Manual for the beck depression inventory-ii*. 1996, San Antonio, TX: Psychological Corporation.
66. Van der Does, A., *Handleiding bij de nederlandse versie van beck depression inventory - second edition (bdi-ii-nl). [manual for the dutch version of the beck depression inventory - second edition (bdi-ii-nl).]*. 2002, Amsterdam: Harcourt.
67. Kovacs, M., *The children's depression, inventory (cdi).* Psychopharmacol Bull, 1985. **21**(4): p. 995-8.
68. R Core Team, *R: A language and environment for statistical computing*. 2019, Vienna, Austria: R Foundation for Statistical Computing.
69. Alexander, A.L., et al., *Diffusion tensor imaging of the brain.* Neurotherapeutics, 2007. **4**(3): p. 316-29.
70. Hasan, K.M., A.L. Alexander, and P.A. Narayana, *Does fractional anisotropy have better noise immunity characteristics than relative anisotropy in diffusion tensor mri? An analytical approach.* Magn Reson Med, 2004. **51**(2): p. 413-7.
71. Budde, M.D., et al., *Axial diffusivity is the primary correlate of axonal injury in the experimental autoimmune encephalomyelitis spinal cord: A quantitative pixelwise analysis.* J Neurosci, 2009. **29**(9): p. 2805-13.
72. Song, S.K., et al., *Demyelination increases radial diffusivity in corpus callosum of mouse brain.* Neuroimage, 2005. **26**(1): p. 132-40.
73. Horsfield, M.A. and D.K. Jones, *Applications of diffusion-weighted and diffusion tensor mri to white matter diseases - a review.* NMR Biomed, 2002. **15**(7-8): p. 570-7.
74. Kochunov, P., et al., *Relationship between white matter fractional anisotropy and other indices of cerebral health in normal aging: Tract-based spatial statistics study of aging.* Neuroimage, 2007. **35**(2): p. 478-87.
75. Smith, S.M., et al., *Advances in functional and structural mr image analysis and implementation as fsl.* Neuroimage, 2004. **23 Suppl 1**: p. S208-19.
76. Andersson, J.L., S. Skare, and J. Ashburner, *How to correct susceptibility distortions in spin-echo echo-planar images: Application to diffusion tensor imaging.* Neuroimage, 2003. **20**(2): p. 870-88.
77. Smith, S.M., *Fast robust automated brain extraction.* Hum Brain Mapp, 2002. **17**(3): p. 143-55.
78. Andersson, J.L.R. and S.N. Sotiropoulos, *An integrated approach to correction for off-resonance effects and subject movement in diffusion mr imaging.* Neuroimage, 2016. **125**: p. 1063-1078.
79. Bastiani, M., et al., *Automated quality control for within and between studies diffusion mri data using a non-parametric framework for movement and distortion correction.* Neuroimage, 2019. **184**: p. 801-812.
80. Behrens, T.E.J., et al., *Characterization and propagation of uncertainty in diffusion-weighted mr imaging.* Magnetic Resonance in Medicine, 2003. **50**(5): p. 1077-1088.
81. Andersson, J.L.R., M. Jenkinson, and S. Smith, *Non-linear registration, aka spatial normalisation*, in *FMRIB technical report TR07JA2*. 2007b, FMRIB Analysis Group of the University of Oxford: Oxford.
82. Andersson, J.L.R., M. Jenkinson, and S. Smith, *Non-linear optimisation*, in *FMRIB technical report TR07JA1*. 2007a, FMRIB Analysis Group of the University of Oxford: Oxford.
83. Rueckert, D., et al., *Nonrigid registration using free-form deformations: Application to breast mr images.* IEEE Trans Med Imaging, 1999. **18**(8): p. 712-21.
84. Acheson, A., et al., *Reproducibility of tract-based white matter microstructural measures using the enigma-dti protocol.* Brain Behav, 2017. **7**(2): p. e00615.
85. Mori, S., et al., *Mri atlas of human white matter*. 2005, Amsterdam: Elsevier.
86. Westlye, L.T., et al., *Error-related negativity is mediated by fractional anisotropy in the posterior cingulate gyrus--a study combining diffusion tensor imaging and electrophysiology in healthy adults.* Cereb Cortex, 2009. **19**(2): p. 293-304.
87. Burkhouse, K.L., et al., *Neural correlates of rumination in adolescents with remitted major depressive disorder and healthy controls.* Cogn Affect Behav Neurosci, 2017. **17**(2): p. 394-405.
88. Ganjgahi, H., et al., *Fast and powerful genome wide association of dense genetic data with high dimensional imaging phenotypes.* Nat Commun, 2018. **9**(1): p. 3254.
89. Ganjgahi, H., et al., *Fast and powerful heritability inference for family-based neuroimaging studies.* NeuroImage, 2015. **115**: p. 256-68.
90. Tissier, R., et al., *Secondary phenotype analysis in ascertained family designs: Application to the leiden longevity study.* Stat Med, 2017. **36**(14): p. 2288-2301.

91. Kendler, K.S. and C.A. Prescott, *Genes, environment and psychopathology*. 2006, New York, NY: The Guilford Press.

92. Kochunov, P., et al., *Heritability of complex white matter diffusion traits assessed in a population isolate.* Hum Brain Mapp, 2016. **37**(2): p. 525-35.

93. Alves, P.N., et al., *An improved neuroanatomical model of the default-mode network reconciles previous neuroimaging and neuropathological findings.* Commun Biol, 2019. **2**: p. 370.

94. Makris, N., et al., *Segmentation of subcomponents within the superior longitudinal fascicle in humans: A quantitative, in vivo, dt-mri study.* Cereb Cortex, 2005. **15**(6): p. 854-69.

95. Parr, T. and K.J. Friston, *The active construction of the visual world.* Neuropsychologia, 2017. **104**: p. 92-101.

96. Barbeau, E.B., M. Descoteaux, and M. Petrides, *Dissociating the white matter tracts connecting the temporo-parietal cortical region with frontal cortex using diffusion tractography.* Sci Rep, 2020. **10**(1): p. 8186.

97. Thiebaut de Schotten, M., et al., *A lateralized brain network for visuospatial attention.* Nat Neurosci, 2011. **14**(10): p. 1245-6.

98. Vossel, S., J.J. Geng, and G.R. Fink, *Dorsal and ventral attention systems: Distinct neural circuits but collaborative roles.* Neuroscientist, 2014. **20**(2): p. 150-9.

99. Jones, D.K., T.R. Knosche, and R. Turner, *White matter integrity, fiber count, and other fallacies: The do's and don'ts of diffusion mri.* Neuroimage, 2013. **73**: p. 239-54.

100. Alexander, A.L., et al., *Characterization of cerebral white matter properties using quantitative magnetic resonance imaging stains.* Brain Connect, 2011. **1**(6): p. 423-46.

101. Feldman, H.M., et al., *Diffusion tensor imaging: A review for pediatric researchers and clinicians.* J Dev Behav Pediatr, 2010. **31**(4): p. 346-56.

102. Thomason, M.E. and P.M. Thompson, *Diffusion imaging, white matter, and psychopathology.* Annu Rev Clin Psychol, 2011. **7**(1): p. 63-85.

103. Haber, S.N., et al., *Circuits, networks, and neuropsychiatric disease: Transitioning from anatomy to imaging.* Biol Psychiatry, 2020. **87**(4): p. 318-327.

104. Bas-Hoogendam, J.M. and P.M. Westenberg, *Imaging the socially-anxious brain: Recent advances and future prospects.* F1000Res, 2020. **9**.

105. Kim, Y.K. and H.K. Yoon, *Common and distinct brain networks underlying panic and social anxiety disorders.* Prog Neuropsychopharmacol Biol Psychiatry, 2018. **80**(Pt B): p. 115-122.

106. Kim, S.Y., et al., *Neural evidence for persistent attentional bias to threats in patients with social anxiety disorder.* Soc Cogn Affect Neurosci, 2018. **13**(12): p. 1327-1336.

107. Owen, M.J., *New approaches to psychiatric diagnostic classification.* Neuron, 2014. **84**(3): p. 564-71.

108. Kochunov, P., et al., *Fractional anisotropy of water diffusion in cerebral white matter across the lifespan.* Neurobiol Aging, 2012. **33**(1): p. 9-20.

109. Wechsler, D., D. Coalson, and S. Raiford, *Wais-iv technical and interpretive manual*. 2008, San Antonio, TX: Pearson.

110. Wechsler, D., *Manual for the wechsler intelligence scale for children - third edition (wisc-iii)*. 1991, San Antonio, TX: The Psychological Corporation.

111. IBM Corp., *Ibm spss statistics for windows, version 25.0*. 2017, IBM Corp.: Armonk, NY.

112. Miers, A.C., et al., *Interpretation bias and social anxiety in adolescents.* J Anxiety Disord, 2008. **22**(8): p. 1462-71.

113. Roelofs, J., et al., *Norms for the beck depression inventory (bdi-ii) in a large dutch community sample.* Journal of Psychopathology and Behavioral Assessment, 2012. **35**(1): p. 93-98.

114. Galvan, A., *Neural plasticity of development and learning.* Hum Brain Mapp, 2010. **31**(6): p. 879-90.

115. Li, X., et al., *The first step for neuroimaging data analysis: Dicom to nifti conversion.* J Neurosci Methods, 2016. **264**: p. 47-56.

116. Koyuncu, A., et al., *The clinical impact of mood disorder comorbidity on social anxiety disorder.* Compr Psychiatry, 2014. **55**(2): p. 363-9.